

Study of mechanical behavior of structures welded with Friction Spot Stir process

Mokhtar Zemri, Benattou Bouchouicha, Mohamed Merzoug and Mohamed Mazari

Abstract—The objective of this study was to show the effects of parameters of Friction Stir Spot Welding process on the temperature measured at 12 and 15 mm from the center of the welding joint of aluminum alloy 6060 T5 and to see also the effects on the mechanical behavior in order to determine parameters used to optimize the mechanical strength of welds. Mechanical properties were determined using tension-shear tests on thin sheet metal assemblies.

Keywords— Failure modes, FSSW, plunge speed, rotation tool, temperature.

I. INTRODUCTION

FRICITION Stir Welding (FSW) is a solid-state welding process firstly introduced by TWI in Cambridge, England and patented in 1991 [1]. In this welding process, a rotating tool is driven into the material and translated along the interface of two or more plates. Friction heats the material which is extruded around the tool and forged by the large pressure produced by the tool shoulder.

Friction Stir Spot Welding (FSSW) is a similar process than FSW and generally applied to aluminum and its alloys in automobile manufacturing [2-3]. This process allows welding superimposed plates. Unlike linear welding, the pin does not move longitudinally, as shown in the Fig. 1 [4]. The tool in rotation, penetrates completely the upper sheet and partially the lower sheet (step a/ and b/. The pin allows mixing at the interface of the sheets providing the metallic bond (step b/). In the End of the cycle, the tool is retracted leaving a welded crown around its footprint (step c/).

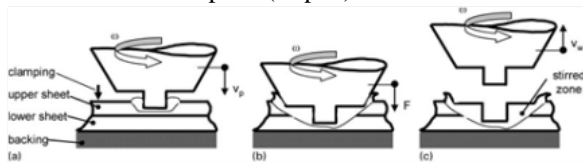


Fig. 1 Principle of welding by FSSW [4].

II. EXPERIMENTAL PROTOCOL

A. Material used

Mokhtar Zemri, Benattou Bouchouicha, Mohamed Merzoug, Mohamed Mazari are with Laboratory of Materials and Reactive Systems – LMSR – University of Sidi Bel Abbès, Algeria. (Corresponding author's phone: +213555112519; e-mail: mzemri@univ-sba.dz.)

TABLE I
CHEMICAL COMPOSITION (%)

%	Si	Fe	Cu	Mn	Mg	Cr	Zn	Ti
Min	0.03	0.10			0.35			
Max	0.60	0.30	0.10	0.10	0.60	0.05	0.15	0.10

TABLE II
MECHANICAL AND PHYSICAL PROPERTIES

E (MPa)	Rp (MPa)	Rm (MPa)	A (%)	v
69500	110	150	14	0.33
d (g/cm ³)	Fusion T° (°C)	λ (W/m°C)	Cp (J/Kg°C)	Hardness (HV)
2.70	605-665	200	945	90

B. Welding tool

Welds were made using a mixing tool, Fig. 2, in a high-alloy steel (X210Cr12) with a threaded cylindrical pin (5 mm diameter and 3.95 mm in length) and a concave shoulder (14 mm diameter). Table III gives the chemical composition of this material.

TABLE III
CHEMICAL COMPOSITION (%) (X210CR12)

C	Si	Mn	P max.	S max.	Cr
1.9 to 2.2	0.1 to 0.6	0.2 to 0.6	0.03	0.03	11 to 13

Mechanical properties are: Rm = 870 MPa and hardness = HB 30 - HRC 58-633

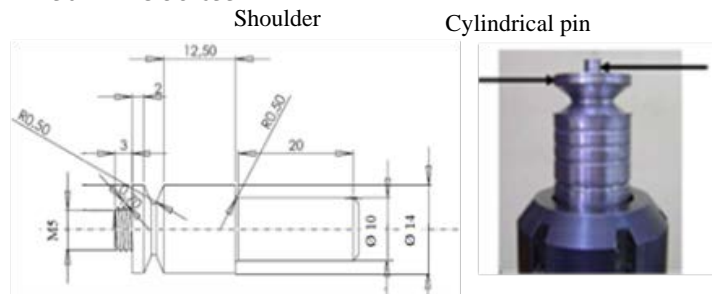


Fig. 2 Tool for Friction Stir Spot Welding

C. Welding parameters

Rotation speed, plunge speed and dwell time were studied. Table 4 lists the parameters used for all welding FSSW process. We varied the tool penetration speed into the material to be welded from 16 to 31.5 mm/min and the tool rotation speed from 1000 to 2000 rpm.

TABLE IV
 WELDING PARAMETERS WITH FSSW

N°	welding speed (mm/min)	Rotational speed rpm	N°	welding speed (mm/min)	Rotational speed rpm
01	16	1000	07	25	1400
02	20	1000	08	31.5	1400
03	25	1000	09	16	2000
04	31.5	1000	10	20	2000
05	16	1400	11	25	2000
06	20	1400	12	31.5	2000

D. Cycle welding time

Fig. 3 shows the course of a cycle welding time in FSSW process. During the entire cycle, rotation speed remains constant and time varies depending on the tool penetration speed. The cycle time of the welding comprises: diving time which depends on the selected welding speed and the thickness of the sheets to be joined, a holding time in order to promote the mixing and a time of removal at the end of the welding operation.

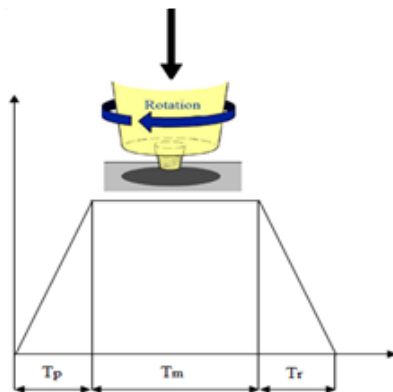


Fig. 3 Schematic description of a FSSW cycle
 Tp: tool plunge, Tm: dwell time and Tr: removal time.

E. Temperature measurement

To measure the temperatures reached during the welding cycle, we used thermocouples, placed approximately at 12 mm and 15 mm from center of stir zone, Fig. 4.

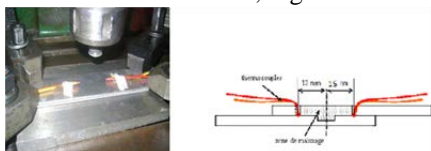


Fig. 4 Thermocouples position.

III. RESULTS AND DISCUSSIONS

A. Microhardness profile

Fig. 5 shows the evolution of the hardness for different plunging speeds V_p and different rotations speed ω . We observe a decrease of the microhardness in the HAZ and hardening in the TMAZ and the MZ [5]. The decrease of the microhardness is due to a small heat distortion during welding, which increases the density of dislocations.

Fig. 6 illustrates the variation of the HV of the nugget compared to base metal according speed rotation and plunging speed. We remark a stable values obtained with 1000 rpm/min and 16mm/min. This stability can satisfy the welded assembly [6].

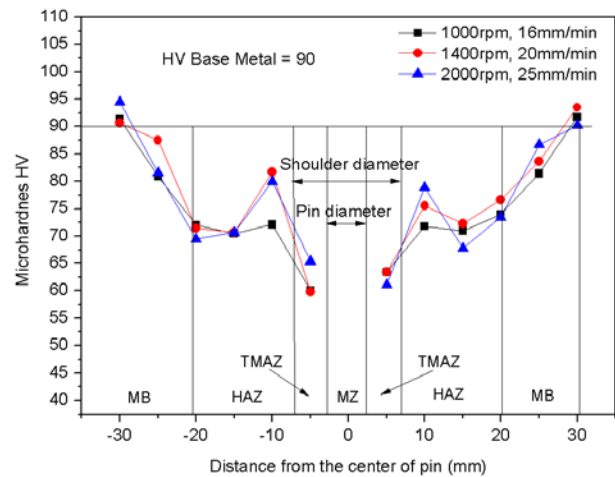


Fig. 5 Variation in microhardness vs. distance

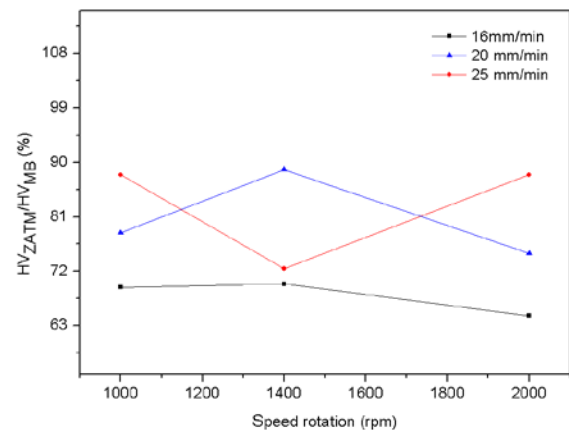
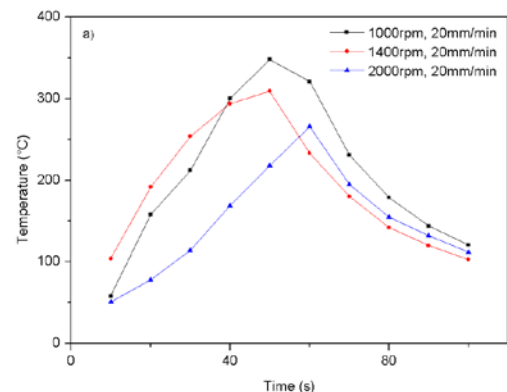


Fig. 6 $HV_{\text{noyau}}/HV_{MB}$ vs. Rotation speed

B. Temperature measurement

Fig. 7 shows the evolution of temperature versus time for the following parameters:

- We can see that the evolution of the temperature is substantially identical for all chosen settings.
- For measurements taken at 12 mm from center of stir zone, Fig. 7a, the maximum temperature is for 1000 rpm, 20 mm/min and the minimum is estimated for 2000 rpm, 20 mm/min.
- For measurements taken at 15 mm from center of stir zone, Fig. 7b, the maximum temperature is for 1400 rpm, 20 mm/min and the minimum is estimated for 1000 rpm, 20 mm/min [6].



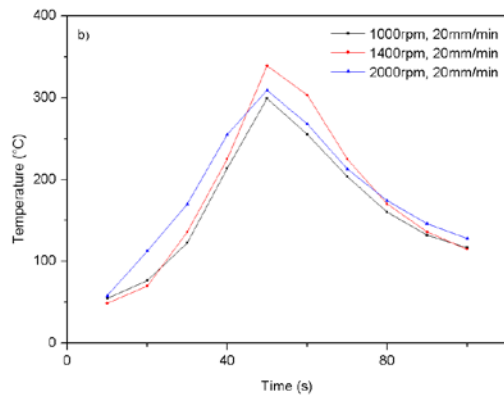


Fig. 7 mixing temperature vs. time

Fig. 8 shows temperature profiles obtained from a constant tool rotation speed equal to 1000 rpm/min and penetration speeds equal to 16, 20, 25 and 31.5 mm/min. We observe that the evolution is identical to that seen previously and the lowest are obtained for 1000 tr/min, 16 mm/min.

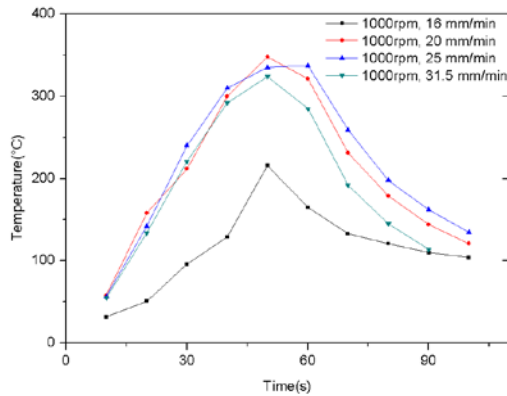


Fig. 8 Temperature profiles for different Feed Rates with a constant rotation speed.

Variation of temperature according to the ratio w^2/v

The dimensions of the mixing tool play a very important role in the production of source of heat during welding. The increase in the ratio w/v contributes to an increase in temperature, Fig. 9. Arbegast et Hartley [7, 8] have developed a parameter (w^2/v : pseudo heat index). The general relationship between the maximum temperature and FSW parameters is expressed by the following formula:

$$T_{max}/T_f = K(w^2/V \cdot 10^4)^\alpha$$

For 6060-T5: $T_f = 600^\circ\text{C}$, $\alpha = 0.05$ and $K = 0.7$

$$T_{max} = 223.43(w^2/V)^{0.05}$$

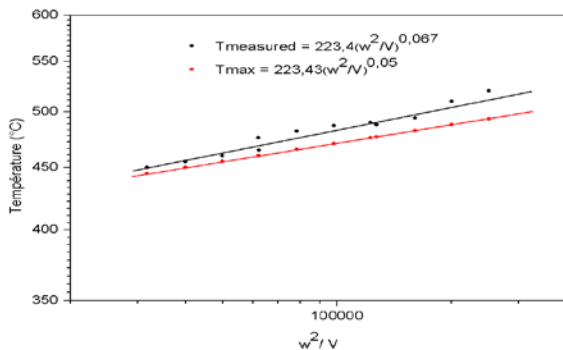


Fig. 9 Temperature vs. w^2/v Estimation and experimental results

C. Tension-shear tests

Fig. 10 shows the geometry of the specimen used for tensile-shear test

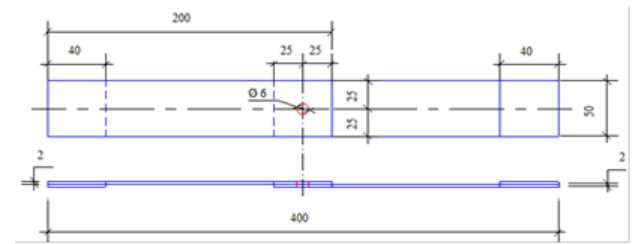


Fig. 10 tensile-shear testing specimen

Fig. 11 shows different assemblies used.



Fig. 11 Different welded specimens

D. Influence of welding parameters

i) Mechanical strength according to rotation speed and plunge speed

Mechanical strength of spot welded by FSSW process is depending on selected parameters, which are rotation speed and plunge speed. For all tests on welded plates with the following parameters: 1000 rpm, 16mm/min; 1400 rpm, 20mm/min and 2000 rpm, 25mm/min, Fig. 10 and 11 show that the maximum load is for low parameters, 1000 rpm and 16 mm/min and begins to decrease until it reaches a minimum value for 2000 rpm and 16 mm/min.

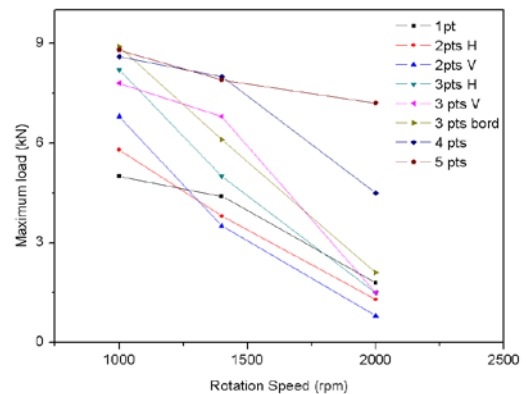


Fig. 12 Effect of the rotation speed on mechanical strength

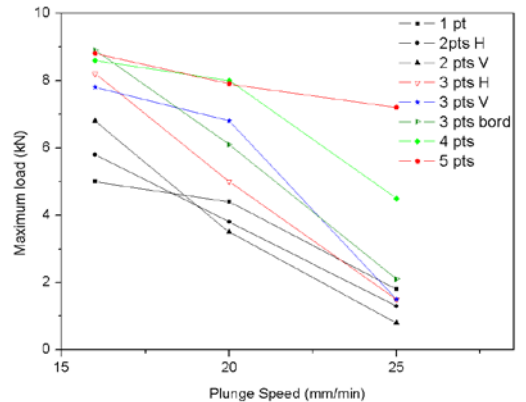


Fig.13 Effect of the rotation plunge speed on mechanical strength

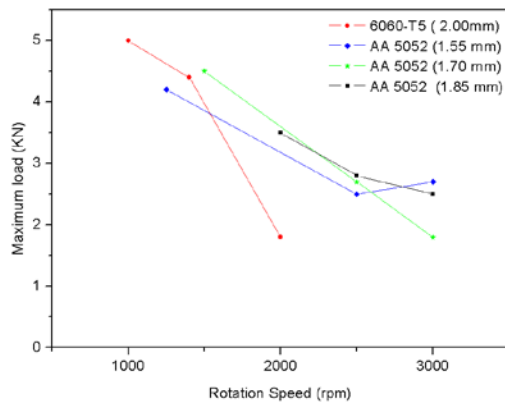


Fig. 14 Mechanical strength vs. Rotation Assembly with 1 point; 6060- T5 and AA 5052 [9]

The rotation speed remains the most influential parameter on the mechanical strength. For plates in 5052 aluminum with 1mm thickness, the maximum load increased from 2.5 kN to 4.2 kN for 2500 rpm and 1250 rpm [9]. We note that there is a little difference between our material and AA5052 alloy, Fig. 14. The first have a good quality welding for low rotation speeds but the second needs high speeds. So the two alloys behave differently at hot, so we can predict that the raising temperature is related to the rotational speed of the pin.

E. Failure mode

In tests shear Lathabai [10] and Tozaki [11] showed that the friction stir welding presents two failure modes. The first is the shear fracture or the interfacial fracture which comes from the transition point and propagates to the free edge of the hole of the pin of the tool and the second is the mixed mode fracture. Fig. 15 illustrates the main failure modes of some welded assemblies by friction stir spot with different parameters.

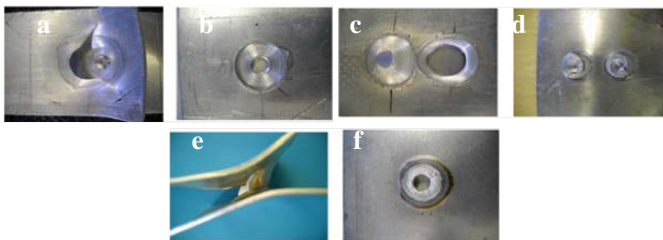


Fig. 15 Different failure modes observed

Fig. 15a shows that the deformation has not occurred in the weld interface, total shear started on the side of the melting zone in the heat affected zone. The upper plate is completely separated from the lower plate.

There is a failure mode caused during the tensile test , Fig. 15d and 15e.

So there was a tear in the upper plate edge of the weld zone. Fig. 15f shows the bottom view where the shear zone is clearly observed.

i) Analysis of rupture zones

Fig. 16 illustrates an example of a shear zone of the upper plate and the lower plate assembly with a point.

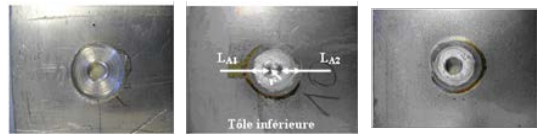


Fig. 16: Transition point and shear mode 1 point (1000rpm - 16mm/min)

The fracture zone in mixed mode S_{cm} , Fig. 16c, is approximately equal to the cylindrical region with a radius $r + L_A$ and L_B a height equal to $(L_{B1}+L_{B2})/2$.

$$S_{cm} = 2\pi(r + L_A).L_E$$

With $L_B = 0.95$ mm, $S_{cm} = 29.83$ mm².

Results of all assemblies are given in tables V and VI.

TABLE V SHEARED SURFACES (mm²) ACCORDING TO THE ROTATION SPEED

Rotation Speed	1pt	2pts H	2pts V	3pts H	3pts V	5pts
1000	58.87 $L_A=2.5$ mm	58.87 $L_A=2.5$ mm	58.87 $L_A=2.5$ mm	58.87 $L_A=2.5$ mm	58.87 $L_A=2.5$ mm	58.87 $L_A=2.5$ mm
1400	75.36 $L_A=3$ mm	58.87 $L_A=1.1$ mm	58.87 $L_A=2.5$ mm	37.09 $L_A=1.75$ mm	58.87 $L_A=2.5$ mm	58.87 $L_A=2.5$ mm
2000	58.87 $L_A=2.5$ mm	58.87 $L_A=2.5$ mm	58.87 $L_A=2.5$ mm	26.9 $L_A=1.35$ mm	58.87 $L_A=2.5$ mm	58.87 $L_A=1$ mm

TABLE VI SHEARED SURFACES IN MIXED MODE (MM²) ACCORDING TO THE ROTATION SPEED

Rotation Speed	1pt	2pts H	2pts V	3pts H	3pts V	5pts
1000	27.63 $L_B=0.88$ mm	12.56 $L_B=0.4$ mm	29.83 $L_B=0.9$ 5mm	29.83 $L_B=0.95$ mm	29.83 $L_B=0.9$ 5mm	29.83 $L_B=0.9$ 5mm
1400	30.39 $L_B=0.88$ mm	13.56 $L_B=0.6$ mm	15.7 $L_B=0.5$ mm	25.35 $L_B=0.95$ mm	29.83 $L_B=0.9$ 5mm	29.83 $L_B=0.9$ 5mm
2000	27.63 $L_B=0.88$ mm	18.84 $L_B=0.6$ mm	15.7 $L_B=0.5$ mm	22.96 $L_B=0.95$ mm	29.83 $L_B=0.9$ 5mm	20.88 $L_B=0.9$ 5mm

ii) Evolution of the shear stress

Shear stress is expressed by: $\tau = F_{max}/S_c$.

Calculated values are given in tables VII and VIII.

TABLE VII SHEAR STRESS (N/mm²) ACCORDING TO THE ROTATION SPEED

Rotation Speed	1pt	2pts H	2pts V	3pts H	3pts V	5pts
1000	8.49	9.85	11.55	13.92	13.24	14.94
1400	5.83	6.45	5.94	13.48	11.55	13.41
2000	3.05	2.20	1.35	5.57	2.54	12.23

TABLE VIII SHEAR STRESS IN MIXED MODE (N/mm²) ACCORDING TO THE ROTATION SPEED

Rotation Speed	1pt	2pts H	2pts V	3pts H	3pts V	5pts
1000	18.09	46.17	22.79	27.48	26.14	29.50
1400	14.47	28.02	22.29	19.72	22.79	26.48
2000	6.51	6.90	5.09	6.53	15.25	34.48

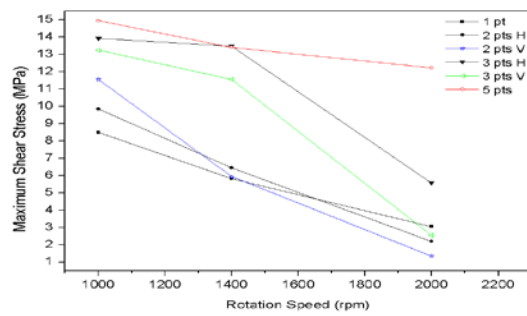


Fig. 17 Effect of the rotation speed on shear stress

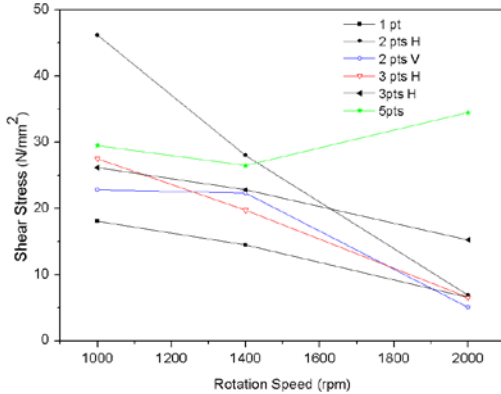


Fig. 18 Effect of the rotation speed on shear stress in mixed mode

Curves in Figures 17 and 18 shows that the speed plays a very important role. When speed decrease. Shear stress becomes important. A significant drop in stress is observed when increasing the rotation speed except for the case of the assembly with 5 points (2000 rpm. 25mm/min)

IV. CONCLUSION

The study of Friction Stir Spot Welding process allowed us to highlight the potential for the realization of spot welds in thin sheet aluminum alloy 6060-T5.

The main objectives of this study were to understand the mechanisms involved during welding and the relationship between the shapes of the mixing zone and the mechanical properties of welds in order to optimize their performance.

For this purpose, a parametric study is centered on the influence of the major factors: the Tool Rotation Speed, the Feed Rate and the Welding Time on the evolution of the temperature and the mechanical behavior of the welds.

Important conclusions were derived from this study:

- The increase in the ratio: rotation speed / plunge speed contributes to the increase in temperature.
- Tensile tests have shown that the sample with 1000 rpm and 16mm/min has good welding quality.

The quality of the welded joint is better when rotation speed is reduced and feed rate is increased.

REFERENCES

[1] W.M. Thomas, E.D. Nicholas, J.C. Needam, M.G. Murch, P. Templesmith, C.J. Dawes. GB Patent Application No. 9125978.8, December 1991 and US Patent No. 5460317, October 1995.

[2] James. M. James et M Mahoney. Proc. 1st International on friction stir welding. Thousand Oaks. California. USA. June 1999

[3] Skrotzki. B. Skrotzki et J. Mucken. Proceedings from Materials Solutions Conference. Indianapolis. IN. ASM International. November 2001

[4] C. Herbelot. T. D. Hoang. A. Imad and N. Benseddq. Damage mechanisms under tension shear loading in friction stir spot welding. Science and Technology of Welding and Joining 2010 VOL 15 NO 8 692

[5] D.A. Wang. S.C. lee. "Microstructures and failure mechanisms of Friction Stir Spot Welds of aluminium 6061-T6 sheets". Journal of Materials Processing Technology. vol. 186. 2007

[6] M. Merzoug. M. Mazari. L. Berrahal and A. Imad: 'Parametric studies of the process of friction spot stir welding of aluminium 6060-T5 alloys'. Mater. Des. 2010. 31. (6). 3023-3028.

[7] R.S. Mishra. Z.Y. Ma. 2005. Friction stir welding and processing. Materials Science and Engineering. 50. 1-78.

[8] Midling. O.T. Milding. J.S. Kvale et O. Dahl. Proc. 1st International on friction stir welding. Thousand Oaks. California. USA. June 1999

[9] H.J. Liu. H. Fujii. M. Maeda. K. Nogi. "Tensile properties and fracture locations of friction-stir-welded joints of 2017-T351 aluminium alloy". Journal of Materials. Proceeding Technology. vol. 142. 2003. p. 692-696.

[10] S. Lathabai. M.J. Painter. G.M.D. Cantin. V.K. Tyagi. "Friction spot joining of an extruded Al-Mg-Si alloy". Scripta Materialia. vol. 55. 2006. p. 899-902.

[11] Y. Tozaki. Y. Uematsu. K. Tokaji. "Effect of tool geometry on microstructure and static strength in friction stir spot welded aluminium alloys". International Journal of Machine Tools and Manufacture. vol. 47. 2007. p. 2230-2236.